Physics of the Dark Universe 52 (2026) 102283

Contents lists available at ScienceDirect

Physics of the Dark Universe

journal homepage: www.elsevier.com/locate/dark

Revisiting ΛCDM extensions in light of re-analyzed CMB data

Jacobo Asorey [a,*], Javier de Cruz Pérez [b]

[a] Departamento de Física Teórica, Centro de Astropartículas y Física de Altas Energías (CAPA), Universidad de Zaragoza, Zaragoza, 50009, Spain
[b] Departamento de Física, Universidad de Córdoba, Campus Universitario de Rabanales, Ctra. N-IV km, 396, Córdoba, 14071, Spain

ARTICLE INFO

Keywords:
Cosmology
Dark-energy
Cosmic microwave background radiation
Large-scale structure

ABSTRACT

In the last years with the increasing precision in cosmological observations we have been able to establish a standard model of cosmology, the so-called ΛCDM, but also find some tensions between cosmological probes that are difficult to explain within the context of this model. We tested several phenomenological extensions of the ΛCDM with the newest datasets from the chain CMB + BAO + SNIa, to see whether they are able to alleviate the aforementioned tensions. We find that when the updated version of the Planck CMB likelihood (PR4 `LoLLiPoP` and `HiLLiPoP`), with respect to the more used likelihoods (PR4 `CamSpec` and PR3), is considered, the lensing anomaly is reduced, and the preference for $A_L > 1$ and $\Omega_k < 0$ is less significant. From the CMB + BAO + SNIa dataset, in the context of the parameterization $w_0 w_a$CDM, we find a preference for a time-evoling dark energy over the rigid cosmological constant which is consistent with the most recent results from DESI collaboration.

1. Introduction

The combination of different cosmological probes during the last decades has led to the rise of a standard model of cosmology, the ΛCDM. This model can describe simultaneously the early universe from cosmic microwave background radiation [1–3], the observed expansion rate evolution with redshift from type Ia Supernova (SN) probes [4–7], baryonic acoustic oscillations (BAO) measurements [8–14] and lately the study of large-scale structure with the 3x2pt probes via weak lensing [15–17]. Despite its success, there are some observational problems that the cosmological standard model is facing up. In particular, some direct measurements of the local expansion rate and indirect measurements from early universe probes show a tension between measurements of the Hubble-Lemaitre constant [18–21]. Other yet not resolved problems are: the radio cosmic dipole problem [22], the σ_8 tension [23] or the tension between 2D and 3D BAO measurements [24,25]. More recently, the first sets of cosmological results with BAO measurements by the Dark Energy Spectroscopic Instrument Collaboration (DESI) [14,26] and the final release of BAO and SN cosmological results from the Dark Energy Survey (DES) Collaboration [7,27] have shown some preference for an evolving dark energy universe [28]. For earlier works claiming evidence in favor of a dynamical dark energy component see [29–36]. For general reviews on the cosmological tensions and ΛCDM anomalies, see [37–40]. Because of these anomalies and tensions, in the last years there has been also a growth on model-independent test studies of datasets for particular cosmological models [33,41–44]. On the observational side, more observations are needed. There is a strong effort regarding the measurement of H_0 using the distance ladder, mainly by two projects, SH0ES program [45], that uses cepheids for calibration, and CCHP program, that uses three different calibrators (Tip of the red giant branch: TRGB, J-region asymptotic giant branch: JAGB, cepheids) [46]. Alternative observational methods involve the use of gravitational wave binaries or strong lensing as they have different systematics [47–49]. Besides the Hubble constant, some high redshift measurements of the expansion rate have shown some hints of potential deviation from a cosmological constant Λ such as with quasars [50,51], type Ia SN [7] and BAO [14]. Of special importance are single rung measurements such as standard speed-guns [52,53] because they allow us to reduce the level of dependence from calibrators. Regarding the solution from possible theoretical solutions, some simple phenomenological extensions to ΛCDM have been proposed as an explanation for these tensions and anomalies. For example, the lensing anomaly induces a change on the amount of matter in the universe (through a change on the small scales) [54]. The latest official Planck Collaboration likelihood is called PR3 [55] and it has been considered the standard Planck likelihood. Recently, a unified framework (NPIPE) has been applied to both the low frequency maps and high frequency maps of Planck mission [56] that also includes extra data collected by satellite repointings that were not included in the previous releases. The NPIPE maps have been used to build two different approaches to the Planck likelihoods for cosmological parameter estimation, the PR4-`CamSpec` [57] and the combined PR4-`LoLLiPoP` and PR4-`HiLLiPoP` likelihoods [58]. Some studies have recently used the PR4-`LoLLiPoP` and PR4-`HiLLiPoP` in combination with the newest DESI data to update cosmological parameter constraints on for a range of

* Corresponding author.
E-mail address: jasorey@unizar.es (J. Asorey).

https://doi.org/10.1016/j.dark.2026.102283
Received 22 December 2025; Received in revised form 16 March 2026; Accepted 18 March 2026
Available online 20 March 2026

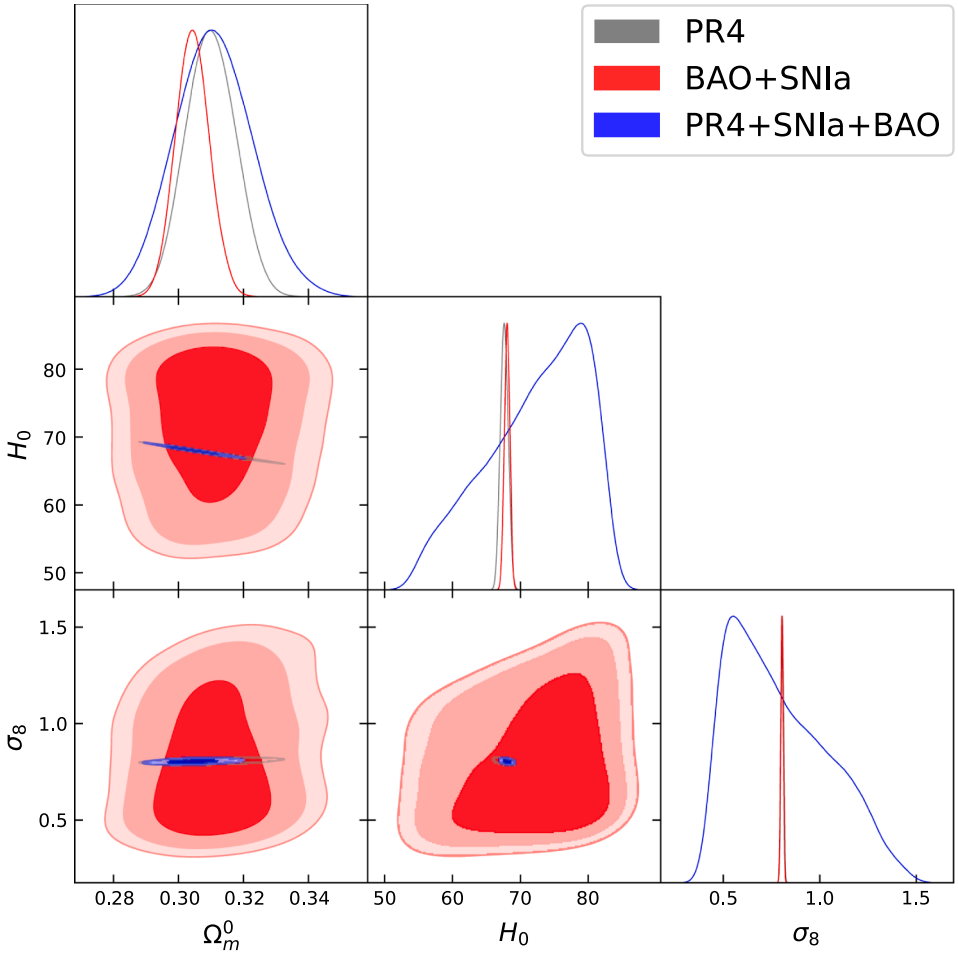

Fig. 1. ΛCDM: Cosmological parameter constraints for the ΛCDM model obtained with the BAO + SNIa, PR4 and PR4 + BAO + SNIa datasets. The parameter H_0 is expressed in km/s/Mpc units.

cosmological models [59,60]. The PR4-CamSpec likelihood for the high-ℓ multipoles of CMB power spectra has been extensively combined with other cosmological probes and for example the DESI Collaboration uses it as default CMB likelihood for the dark energy studies.

However, the combination of the latest Planck likelihood (PR4-LoLLiPoP and PR4-HiLLiPoP) with BAO and SN measurements to study the tensions between the simplest ΛCDM extensions (e.g. Universe spatial curvature as a free parameter) has not been that extensively studied as deeply in the past as other dataset combinations.

In this paper, we use data from PR4 Planck LoLLiPoP and HiLLiPoP likelihood, DESI 2024 BAO data and SNIa from the Pantheon+ sample in order to get constraints in 5 models of cosmology to study the tensions in the parameter constraints. Throughout the paper we refer to PR4 Planck LoLLiPoP and HiLLiPoP likelihood as PR4.

2. Data

To constrain the cosmological parameters that characterize each of the models under study we utilize CMB anisotropy and weak lensing data, BAO and SNIa data. Some details of the different datasets, together with the corresponding references are provided in the following.

PR4: We consider the PR4 updated versions, with respect to the PR3 (which referes to the Planck 2018 TTTEEE data [2]), of the likelihoods that contain the Planck CMB temperature anisotropy and polarization data as well as its corresponding cross-spectra [58]. We refer the readers to that reference, where all the technical details involved in getting the upgraded versions of the HiLLiPoP (hlp) and LoLLiPoP (lol) are provided. In the CMB data combination considered only the low multipole temperature (lowT) likelihood comes from PR3. Following author's notation, the full TTTEEE likelihood is composed by: lowT ($2 \leq \ell \leq 30$) + lolE ($2 \leq \ell \leq 30$) + hlpTTTEEE ($30 \leq \ell \leq 2500$ for TT and for TE and EE $30 \leq \ell \leq 2000$).

(PR4) lensing: The lensing potential power spectrum obtained from the analysis of the Planck CMB PR4 maps [61].

BAO: We employ a total of 12 BAO data points from both anisotropic and isotropic analyses from DESI 2024 [14] spanning the redshift range $0.295 \leq z \leq 2.3330$. The 10 anisotropic data points are embodied in the $D_{\rm M}(z_{\rm eff})/r_d$ and $D_{\rm H}(z_{\rm eff})/r_d$ estimators whereas the 2 isotropic data points are given in the form of the $D_{\rm V}(z_{\rm eff})/r_d$ observable. The values for the different points together with the correlation coefficients for the anisotropic results are provided in Table 1 of [14]. In this work we stick to the use of the 3D BAO data. We recommend [25,36,62] for discussions about the tension between the results obtained with 3D BAO and 2D BAO data.

SNIa: The Pantheon+ compilation [5], contains a total of 1701 measurements of the apparent magnitude of supernova type Ia as a function of the redshift. In order to avoid dependencies of the considered model to deal with the peculiar velocities we remove from the likelihoods all the data points with redshift $z < 0.01$. The remaining 1590 measurements probe the redshift range $0.01016 \leq z \leq 2.26137$. In

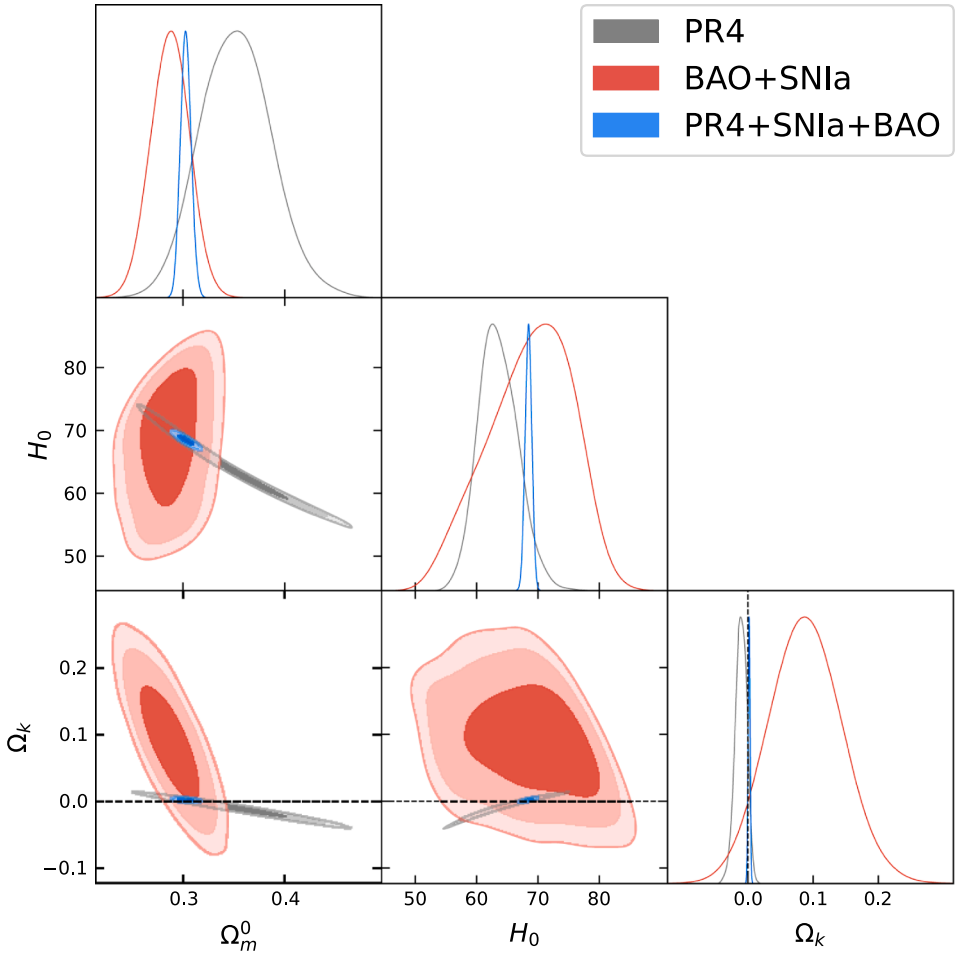

Fig. 2. **ΛCDM** + Ω_k: Cosmological parameter constraints for the ΛCDM + Ω_k model obtained with the BAO + SNIa, PR4 and PR4 + BAO + SNIa datasets. The parameter H_0 is expressed in km/s/Mpc units. We include the dashed lines to highlight the flat Universe case ($\Omega_k = 0$).

Table 1
ΛCDM: Mean and 68% confidence limits of the primary and derived parameters of the ΛCDM model obtained after analyzing the datasets: BAO + SNIa, PR4, PR4 + lensing, PR4 + BAO + SNIa and PR4 + lensing + nonCMB. The H_0 has units of km/s/Mpc whereas r_d has units of Mpc. We also include the values of $\chi^2_{\rm min}$,DIC and p_D.

Parameter	BAO + SNIa	PR4	PR4 + lensing	PR4 + BAO + SNIa	PR4 + lensing + BAO + SNIa
$\Omega_b h^2$	$0.0226^{+0.0120}_{-0.0050}$	0.02223 ± 0.00014	0.02221 ± 0.00014	0.02229 ± 0.00012	0.02229 ± 0.00012
$\Omega_c h^2$	$0.137^{+0.030}_{-0.022}$	0.1188 ± 0.0013	0.1192 ± 0.0012	0.11795 ± 0.00088	0.11817 ± 0.00082
H_0	72^{+10}_{-5}	67.63 ± 0.56	67.49 ± 0.52	68.04 ± 0.39	67.95 ± 0.37
τ	0.0579	0.0579 ± 0.0063	0.0588 ± 0.0062	0.0591 ± 0.0063	0.0608 ± 0.0061
$\ln(10^{10} A_s)$	2.76 ± 0.63	3.039 ± 0.014	3.045 ± 0.012	3.040 ± 0.014	3.049 ± 0.012
n_s	0.9671	0.9671 ± 0.0042	0.9664 ± 0.0041	0.9694 ± 0.0036	0.9689 ± 0.0035
Ω_m	0.311 ± 0.012	0.3099 ± 0.0077	0.3119 ± 0.0071	0.3043 ± 0.0052	0.3056 ± 0.049
σ_8	$0.78^{+0.16}_{-0.34}$	0.8061 ± 0.0066	0.8093 ± 0.0051	0.8039 ± 0.0063	0.8081 ± 0.0050
r_d	$140.6^{+6.6}_{-19}$	147.56 ± 0.27	147.49 ± 0.25	147.73 ± 0.21	147.67 ± 0.20
$\chi^2_{\rm min}$	1418.28	30551.10	30559.38	31969.59	31978.16
DIC	1422.30	30599.64	30608.98	32021.87	32031.64
p_D	2.01	24.27	24.80	26.14	26.74

our analyses the absolute magnitude of supernova, usually denoted by M, is treated as a nuisance parameter.

3. Methodology

The ΛCDM model can be described by six cosmological parameters $\Omega_b h^2$, $\Omega_c h^2$, H_0, τ, A_s and n_s. The Ω_b and Ω_c represent the present values of the baryon and cold dark matter density parameters, H_0 is the current value of the Hubble function, τ is the reionization optical depth and the last two parameters are related with the scalar type primordial power spectrum

$$P_\delta(k) = A_s \left(\frac{k}{k_0}\right)^{n_s} \tag{1}$$

with A_s the amplitude of the power spectrum, n_s the spectral index and $k_0 = 0.05\text{Mpc}^{-1}$ the pivot scale. As our goal is to check the tensions and anomalies between different datasets and re-analysis, we study the standard model of cosmology, the so-called ΛCDM model together with some commonly studied extensions. The background evolution of all the models under study can be generally described by the following expression

Table 2
ΛCDM + Ω_k: Mean and 68% confidence limits of the primary and derived parameters of the ΛCDM + Ω_k model obtained after analyzing the datasets: BAO + SNIa, PR4, PR4 + lensing, PR4 + BAO + SNIa and PR4 + lensing + non-CMB. The H_0 has units of km/s/Mpc whereas r_d has units of Mpc. We also include the values of $\chi^2_{\rm min}$ and DIC together with the differences with respect to the ΛCDM model, denoted by $\Delta\chi^2_{\rm min}$ and ΔDIC, respectively. We include p_D, the effective number of free parameters.

Parameter	BAO + SNIa	PR4	PR4 + lensing	PR4 + BAO + SNIa	PR4 + lensing + BAO + SNIa
$\Omega_b h^2$	$0.0266^{+0.012}_{-0.0049}$	0.02229 ± 0.00014	0.02228 ± 0.00014	0.02221 ± 0.00013	0.02221 ± 0.00013
$\Omega_c h^2$	$0.110^{+0.020}_{-0.028}$	0.1183 ± 0.0013	0.1183 ± 0.0013	0.1190 ± 0.0012	0.1192 ± 0.0012
H_0	69^{+8}_{-6}	$63.6^{+3.0}_{-3.5}$	64.7 ± 2.2	68.46 ± 0.54	68.36 ± 0.53
τ	0.0564	0.0564 ± 0.0062	0.0567 ± 0.0063	0.0579 ± 0.0063	0.0598 ± 0.0061
$\ln(10^{10} A_s)$	2.75 ± 0.62	3.035 ± 0.014	3.035 ± 0.014	3.040 ± 0.014	3.049 ± 0.012
n_s	0.9689	0.9689 ± 0.0043	0.9687 ± 0.0043	0.9667 ± 0.0041	0.9664 ± 0.0041
Ω_k	0.088 ± 0.056	$-0.0107^{+0.0096}_{-0.0080}$	$-0.0073^{+0.0063}_{-0.0052}$	0.0018 ± 0.0015	0.0018 ± 0.0015
Ω_m	0.287 ± 0.019	0.352 ± 0.035	$0.338^{+0.020}_{-0.023}$	0.3028 ± 0.0052	0.3040 ± 0.0051
σ_8	$0.62^{+0.14}_{-0.29}$	0.797 ± 0.010	0.7990 ± 0.0096	0.8079 ± 0.0071	0.8120 ± 0.0059
r_d	$147.2^{+8.7}_{-19}$	147.64 ± 0.27	147.64 ± 0.27	147.53 ± 0.26	147.49 ± 0.26
$\chi^2_{\rm min}$	1415.20	30547.30	30557.39	31965.7	31974.71
$\Delta\chi^2_{\rm min}$	+3.08	+3.80	+1.99	+3.89	+3.45
DIC	1421.24	30601.10	30608.97	32026.91	32034.59
p_D	3.02	26.90	25.79	30.61	29.94
ΔDIC	+1.06	−1.46	+0.01	−2.47	−2.95

Table 3
ΛCDM + A_L: Mean and 68% confidence limits of the primary and derived parameters of the ΛCDM + A_L model obtained after analyzing the datasets: PR4, PR4 + lensing, PR4 + BAO + SNIa and PR4 + lensing + nonCMB. The H_0 has units of km/s/Mpc whereas r_d has units of Mpc. We also include the values of $\chi^2_{\rm min}$ and DIC together with the differences with respect to the ΛCDM model, denoted by $\Delta\chi^2_{\rm min}$ and ΔDIC, respectively. We include p_D, the effective number of free parameters.

Parameter	PR4	PR4 + lensing	PR4 + BAO + SNIa	PR4 + lensing + BAO + SNIa
$\Omega_b h^2$	$0.02228^{+0.00016}_{-0.00015}$	$0.02229^{+0.00016}_{-0.00014}$	$0.02234^{+0.0013}_{-0.0012}$	0.02235 ± 0.00012
$\Omega_c h^2$	0.1184 ± 0.0014	$0.1183^{+0.0013}_{-0.0015}$	0.11762 ± 0.00090	0.11761 ± 0.00089
H_0	67.87 ± 0.65	$67.91^{+0.67}_{-0.60}$	68.21 ± 0.41	68.22 ± 0.41
τ	0.0571 ± 0.0063	0.0572 ± 0.0063	0.0576 ± 0.0064	0.0577 ± 0.0063
$\ln(10^{10} A_s)$	3.036 ± 0.015	3.036 ± 0.015	3.035 ± 0.015	3.036 ± 0.015
n_s	0.9685 ± 0.0046	0.9688 ± 0.0046	0.9705 ± 0.0036	0.9708 ± 0.0036
A_L	1.036 ± 0.055	1.041 ± 0.038	1.051 ± 0.050	1.050 ± 0.035
Ω_m	$0.3069^{+0.0080}_{-0.0093}$	$0.3063^{+0.0077}_{-0.0092}$	$0.3023^{+0.0050}_{-0.0057}$	$0.3022^{+0.0050}_{-0.0056}$
σ_8	0.8034 ± 0.0076	0.8032 ± 0.0076	0.8010 ± 0.0068	0.8012 ± 0.0068
r_d	147.63 ± 0.28	147.65 ± 0.28	147.77 ± 0.21	147.76 ± 0.21
$\chi^2_{\rm min}$	30548.57	30556.30	31968.25	31976.06
$\Delta\chi^2_{\rm min}$	+2.53	+3.08	+1.34	+2.10
DIC	30602.15	30610.84	32022.17	32028.49
p_D	26.79	27.27	26.88	26.22
ΔDIC	−2.51	−1.86	−0.30	+0.92

Table 4
w_0CDM: Mean and 68% confidence limits of the primary and derived parameters of the w_0CDM model obtained after analyzing the datasets: BAO + SNIa, PR4, PR4 + lensing, PR4 + BAO + SNIa and PR4 + lensing + nonCMB. The H_0 has units of km/s/Mpc whereas r_d has units of Mpc. We also include the values of $\chi^2_{\rm min}$ and DIC together with the differences with respect to the ΛCDM model, denoted by $\Delta\chi^2_{\rm min}$ and ΔDIC, respectively. We include p_D, the effective number of free parameters.

Parameter	BAO + SNIa	PR4	PR4 + lensing	PR4 + BAO + SNIa	PR4 + lensing + BAO + SNIa
$\Omega_b h^2$	$0.0266^{+0.012}_{-0.0050}$	0.02227 ± 0.00014	0.02226 ± 0.00013	0.02232 ± 0.00012	0.02231 ± 0.00012
$\Omega_c h^2$	0.121 ± 0.024	0.1186 ± 0.0012	0.1187 ± 0.0011	0.11753 ± 0.00097	0.11791 ± 0.00092
H_0	70^{+9}_{-5}	85^{+10}_{-6}	85^{+10}_{-6}	67.55 ± 0.70	67.58 ± 0.70
τ	0.0576	0.0576 ± 0.0063	0.0579 ± 0.0061	0.0597 ± 0.0064	0.0614 ± 0.0062
$\ln(10^{10} A_s)$	2.75 ± 0.63	3.038 ± 0.014	3.039 ± 0.012	3.041 ± 0.014	3.050 ± 0.012
n_s	0.9678	0.9678 ± 0.0041	0.9677 ± 0.0040	0.9704 ± 0.0037	0.9698 ± 0.0036
w_0	-0.925 ± 0.049	$-1.51^{+0.18}_{-0.35}$	$-1.52^{+0.18}_{-0.33}$	-0.978 ± 0.026	-0.984 ± 0.026
Ω_m	0.299 ± 0.014	$0.204^{+0.017}_{-0.060}$	$0.202^{+0.017}_{-0.058}$	0.3080 ± 0.0068	0.3086 ± 0.0067
σ_8	$0.70^{+0.14}_{-0.31}$	$0.946^{+0.095}_{-0.050}$	$0.950^{+0.089}_{-0.048}$	0.797 ± 0.011	0.8031 ± 0.0092
r_d	$144.4^{+7.6}_{-1.9}$	147.60 ± 0.26	147.58 ± 0.25	147.81 ± 0.23	147.72 ± 0.21
$\chi^2_{\rm min}$	1415.40	30549.08	30557.23	31969.25	31977.40
$\Delta\chi^2_{\rm min}$	+2.88	+2.02	+2.15	+0.34	+0.76
DIC	1421.34	30600.12	30608.87	32022.13	32033.22
p_D	2.97	25.52	25.82	26.44	27.91
ΔDIC	+0.96	−0.48	+0.11	−0.26	−1.58

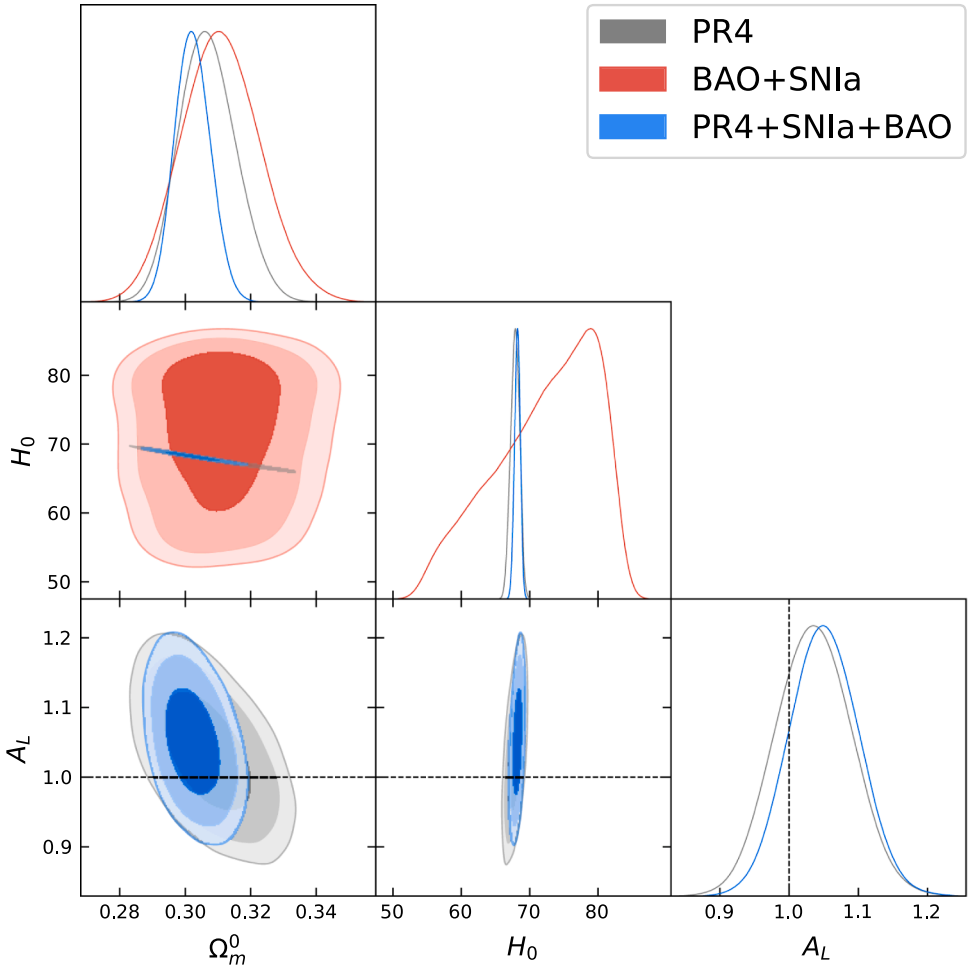

Fig. 3. **ΛCDM** + A_L: Cosmological parameter constraints for the ΛCDM + A_L model obtained with the BAO + SNIa, PR4 and PR4 + BAO + SNIa datasets. The parameter H_0 is expressed in km/s/Mpc units. The dashed lines represent the $A_L = 1$ case.

Table 5
w_0w_a**CDM**: Mean and 68% confidence limits of the primary and derived parameters of the w_0w_aCDM model obtained after analyzing the datasets: BAO + SNIa, PR4, PR4 + lensing, PR4 + BAO + SNIa and PR4 + lensing + non-CMB. The H_0 has units of km/s/Mpc whereas r_d has units of Mpc. We also include the values of $\chi^2_{\rm min}$ and DIC together with the differences with respect to the ΛCDM model, denoted by $\Delta\chi^2_{\rm min}$ and ΔDIC, respectively. We include p_D, the effective number of free parameters.

Parameter	BAO + SNIa	PR4	PR4 + lensing	PR4 + BAO + SNIa	PR4 + lensing + BAO + SNIa
$\Omega_b h^2$	$0.0270^{+0.012}_{-0.0047}$	0.02227 ± 0.00014	0.02227 ± 0.00014	0.02225 ± 0.00013	0.02224 ± 0.00013
$\Omega_c h^2$	0.135 ± 0.032	0.1185 ± 0.0012	0.1185 ± 0.0012	0.1186 ± 0.0011	0.11881 ± 0.00098
H_0	72^{+9}_{-6}	84^{+10}_{-6}	84^{+10}_{-6}	67.84 ± 0.72	67.89 ± 0.72
τ	0.0575	0.0575 ± 0.0062	0.0576 ± 0.0061	0.0580 ± 0.0063	0.0587 ± 0.0061
$\ln(10^{10} A_s)$	2.76 ± 0.63	3.037 ± 0.014	3.038 ± 0.012	3.039 ± 0.014	3.043 ± 0.012
n_s	0.9681	0.9681 ± 0.0041	0.9680 ± 0.0040	0.9678 ± 0.0038	0.9674 ± 0.0037
w_0	$-0.867^{+0.069}_{-0.078}$	$-1.27^{+0.41}_{-0.47}$	-1.28 ± 0.44	-0.849 ± 0.062	-0.843 ± 0.062
w_a	-0.53 ± 0.58	$-1.03^{+0.74}_{-1.8}$	$-1.02^{+0.72}_{-1.80}$	$-0.59^{+0.28}_{-0.25}$	$-0.64^{+0.29}_{-0.24}$
Ω_m	$0.310^{+0.023}_{-0.015}$	$0.209^{+0.016}_{-0.065}$	$0.208^{+0.017}_{-0.065}$	0.3075 ± 0.0069	0.3076 ± 0.0068
σ_8	$0.78^{+0.19}_{-0.35}$	$0.943^{+0.10}_{-0.049}$	$0.945^{+0.10}_{-0.047}$	0.809 ± 0.012	0.8131 ± 0.0098
r_d	$140.9^{+8.2}_{-20}$	147.61 ± 0.26	147.60 ± 0.25	147.60 ± 0.24	147.56 ± 0.22
$\chi^2_{\rm min}$	1414.78	30547.32	30557.44	31964.42	31972.85
$\Delta\chi^2_{\rm min}$	+3.50	+3.78	+1.94	+5.17	+5.31
DIC	1422.62	30601.84	30608.62	32019.50	32028.65
p_D	3.92	27.26	25.59	27.54	27.90
ΔDIC	−0.32	−2.20	+0.36	+2.37	+2.99

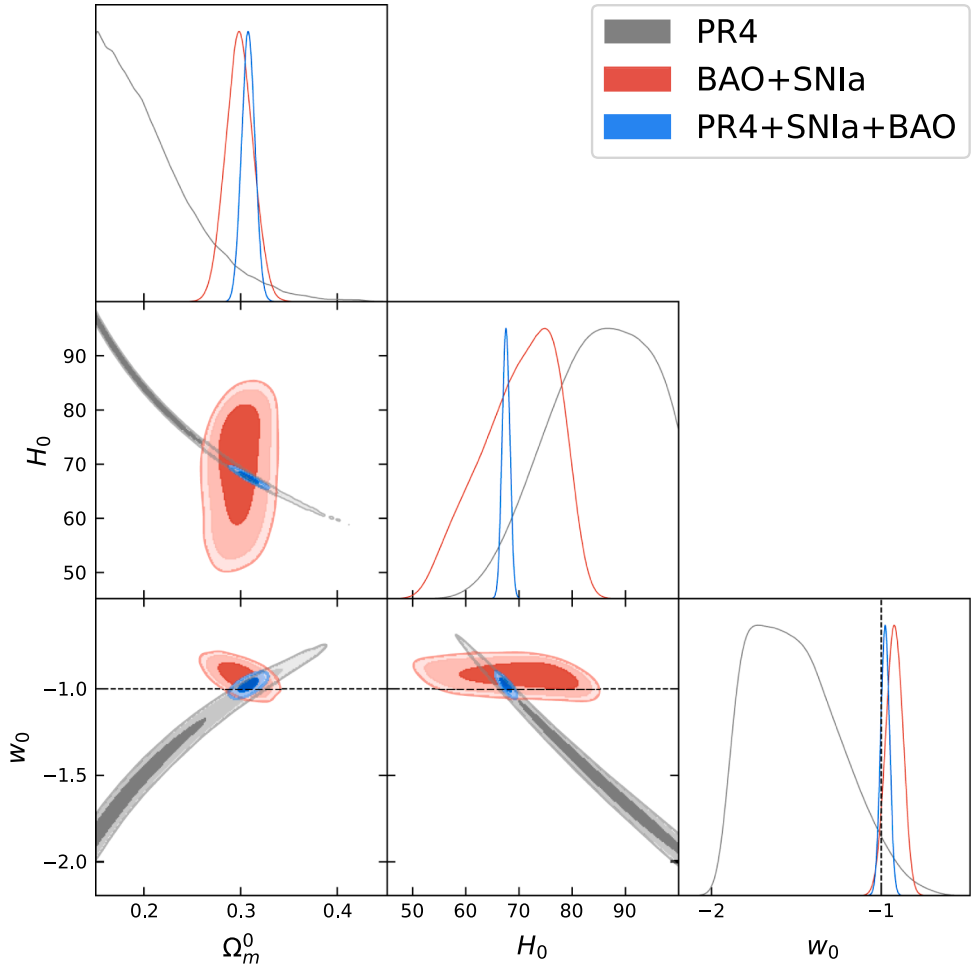

Fig. 4. w_0**CDM**: Cosmological parameter constraints for the w_0CDM model obtained with the BAO + SNIa, PR4 and PR4 + BAO + SNIa datasets. The parameter H_0 is expressed in km/s/Mpc units. The dashed lines highlight the ΛCDM case.

of the Hubble function

$$H^2(a) = H_0^2[\Omega_\gamma a^{-4} + (\Omega_b + \Omega_c)a^{-3} + \Omega_k a^{-2} + \Omega_\nu(a) + \Omega_{\rm DE}(a)]. \tag{2}$$

where Ω_γ represents the present value of the photon density parameter, Ω_k is the curvature parameter, $\Omega_\nu(a)$ encodes the contribution from massive and massless neutrinos and $\Omega_{\rm DE}(a)$ contains the contribution of the dark energy fluid.

ΛCDM + Ω_k: In this model, the spatial hypersurfaces are not assumed to be flat. This implies changes in the calculation of cosmological distances, as well as modifications in the shape of the power spectrum of primordial fluctuations where we assume the same parametrization as the one used by the Planck Collaboration [2,63]:

$$P_\delta(q) \propto \frac{(q^2 - 4K)^2}{q(q^2 - K)^2} A_s \left(\frac{k}{k_0}\right)^{n_s - 1} \tag{3}$$

where $q^2 = k^2 + K^2$ is the wave-number for the non-flat ΛCDM model and $K = -(H_0^2/c^2)\Omega_k$ accounts for the curvature. See [64] for the role of the assumed value of Ω_k in the fiducial cosmology.

ΛCDM + A_L: The CMB photons go through weak lensing scattering during their travel through the large-scale structures of the universe. The CMB lensing is described [65,66] by the power spectrum of the lensing potential $C_\ell^{\psi\psi}$ and the impact on the TT power spectrum of CMB is given by a convolution with the unlensed TT power spectrum C_ℓ. In order to check the consistency of the CMB lensing models, within the context of the ΛCDM, a test parameter A_L was introduced [54] in the lensing power spectrum as $C_\ell^{\psi\psi} \to A_L C_\ell^{\psi\psi}$ so the expression for the lensed CMB TT, $\tilde{C}_\ell$, power spectrum is given by:

$$\tilde{C}_\ell \approx C_\ell + A_L \int \frac{d^2\boldsymbol{\ell'}}{(2\pi)^2} [\boldsymbol{\ell'} \cdot (\boldsymbol{\ell} - \boldsymbol{\ell'})]^2 C^{\psi\psi}_{|\boldsymbol{\ell} - \boldsymbol{\ell'}|} C_{\ell'}. \tag{4}$$

where $A_L = 1$ if the modeling of $C^{\psi\psi}_{|\boldsymbol{\ell} - \boldsymbol{\ell'}|}$ within general relativity is correct. Allowing the phenomenological parameter A_L to vary in our analysis will allow us to check whether the theoretical prediction for the amount of weak lensing in the CMB spectra is correct or not.

w_0**CDM**: This is a simple zero-order parametrization that allows to track a possible time-evolution of the dark energy component. The parameterization is characterized by a constant dark energy equation of state parameter w_0 whose value may in principle deviate from the cosmological constant behavior $w_0 \neq -1$. This can mimic the quintessence ($w_0 > -1$) or phantom ($w_0 < -1$) behavior of a scalar field model, provided that the corresponding equation of state parameter is approximately constant. The cosmological constant contribution is replaced by $\Omega_{\rm DE}(a) = \Omega_\Lambda a^{-3(1+w_0)}$.

$w_0 w_a$**CDM**: This model is the next order parametrization, usually named as Chevallier-Polarski-Linder (CPL) [67,68], with respect to w_0CDM and accounts for the possibility of a scale factor dependence of the dark energy equation of state parameter $w(a) = w_0 + w_a(1 - a)$, which has a well-defined asymptotic limit $w(a \to 0) \simeq w_0 + w_a$ in the early universe. In this case the dark energy density reads

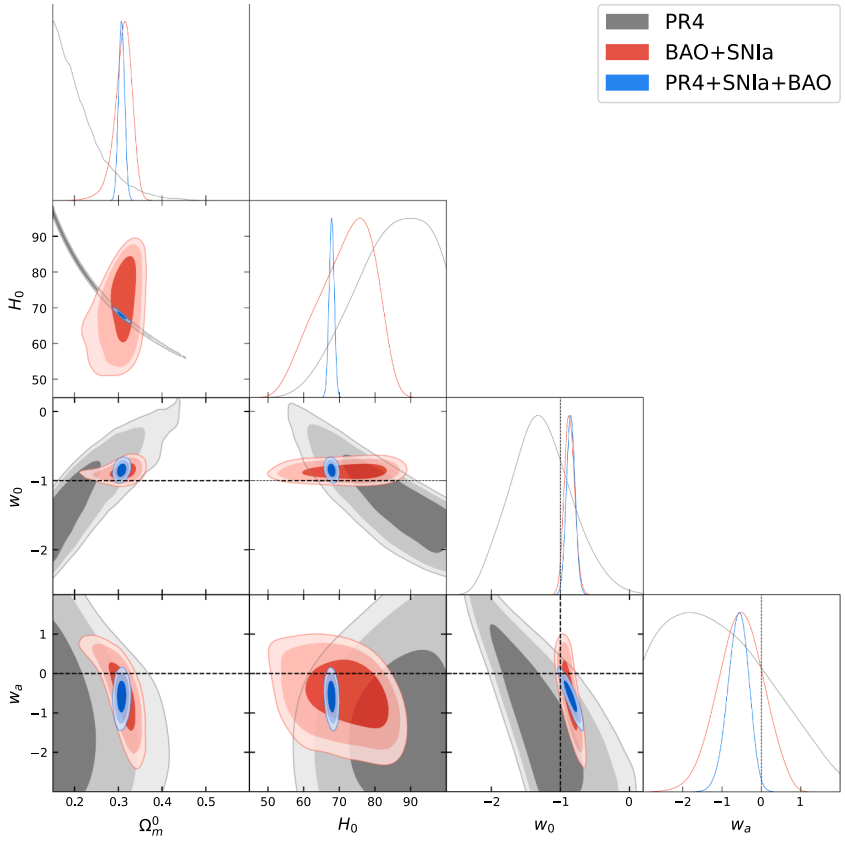

Fig. 5. w_0w_a**CDM**: Cosmological constraints for the w_0w_aCDM model obtained with the BAO + SNIa, PR4 and PR4 + BAO + SNIa datasets. The parameter H_0 is expressed in km/s/Mpc units. The dashed lines in the plot are a reference to the ΛCDM case.

$\Omega_{\rm DE}(a) = \Omega_\Lambda a^{-3(1+w_0+w_a)} e^{-3w_a(1-a)}$. Check [69–73] for alternative dark energy parameterizations.

The performance of the different cosmological models and parameterizations, when it comes to fitting the observation data, is studied through the computation of the joint log-likelihood $\log \mathcal{L}$. Assuming the relation $\chi^2 \propto -2\log\mathcal{L}$, the joint χ^2-function, whose individual components are

$$\chi^2_{\rm tot} = \chi^2_{\rm CMB} + \chi^2_{\rm lensing} + \chi^2_{\rm BAO} + \chi^2_{\rm SNIa} \tag{5}$$

where here, for the sake of simplicity, CMB stands for the TTTEEE likelihood described in the previous section.

The cosmological background and perturbation equations are solved by making use of the Einstein-Boltzmann system solver `CLASS` [74,75] whereas the exploration of the parameter space is carried out through the use of a Markov chain Monte Carlo analysis being the corresponding algorithm implemented in `Cobaya` [76]. As a criterion to ensure that convergence has been reached we use the Gelman-Rubin convergence statistics [77,78] setting the condition to stop the Monte Carlo sampling when $R - 1 < 0.01$. Once the converged chains are obtained we employ the code `GetDist` [79] to get the corresponding posterior distributions. In our analyses we consider conservative flat priors, in particular, for the six primary parameters common to all the models: $0.005 \le \Omega_b h^2 \le 0.1$, $0.001 \le \Omega_c h^2 \le 0.99$, $20 \le H_0[\text{km/s/Mpc}] \le 100$, $0.01 \le \tau \le 0.8$, $0.8 \le n_s \le 1.2$ and $1.61 \le \ln(10^{10}A_s) \le 3.91$. As for the non-standard parameters, while in the case of the ΛCDM + Ω_k model, the curvature parameter varies within the range $-0.5 \le \Omega_k \le 0.5$, for the ΛCDM + A_L the lensing parameter is allowed to vary within $0 \le A_L \le 10$. In regard to the dynamical dark energy parameterizations, for w_0CDM $-3.0 \le \omega_0 < 0.2$ and for $\omega_0\omega_a$CDM $-3.0 \le \omega_0 \le 0.2$ and $-3 \le \omega_a \le 2$. In the tables, in addition to the values of the primary cosmological parameters, we also provide the values of three derived parameters, namely: the total non-relativistic matter density parameter Ω_m which contains the contribution of baryons, cold dark matter and massive neutrinos, σ_8, the root mean square of matter perturbations computed at the scale $R_8 = 8/h$Mpc [1] and r_d, the radius of the sound horizon evaluated at the drag epoch z_d. Finally, we fix the current value of the CMB temperature to $T_0 = 2.7255$ K [82] and we consider three different neutrino species, being two of them massless and one massive with $m_\nu = 0.06$ eV. Since the BAO + SNIa dataset alone is not capable of constraining the parameters τ and n_s, in the corresponding analyses, we fix their values to the ones obtained using the PR4 data. As mentioned before, the parameter A_L is introduced to rescale the lensing power spectrum and consequently it plays a very minor role (only through correlations with other parameters) in the late time universe. Therefore in Table 3 we do not provide the results when only BAO + SNIa data are analyzed since the results are basically the same as the ones obtained for the ΛCDM model.

In order to compare the performance of the different models and parameterizations under study when it comes to fitting the cosmological data somehow we need to penalize the presence of extra parameters. This can be accomplished by making use of the deviance information criterion (DIC) [83–85], which value can be computed with

$$\text{DIC} = \chi^2(\hat\theta) + 2p_D. \tag{6}$$

In the above expression $p_D = \overline{\chi^2} - \chi^2(\hat\theta)$ represents the effective number of parameters (the number can be obtained from the values provided in corresponding tables), with $\overline{\chi^2}$ we denote the average value of the χ^2-

[1] See [80,81] for discussions in favor of using σ_{12} instead of σ_8.

function and $\chi^2(\hat{\theta})$ is the χ^2-function evaluated in the best-fit values of the fitting parameters. The best-fit values are obtained with the BOBYQA minimizer [86,87]. We define the difference between the $\chi^2_{\rm min}$ of a given extended model X and the ΛCDM one as $\Delta\chi^2_{\rm min} = \chi^2_{\rm min,\Lambda CDM} - \chi^2_{\rm min,X}$. We compute differences in the DIC value with respect to the ΛCDM model as

$$\Delta{\rm DIC} = {\rm DIC}_{\Lambda{\rm CDM}} - {\rm DIC}_{\rm X} \tag{7}$$

where the X represents all the non-standard models and parameterizations considered in this work. If we get $\Delta{\rm DIC} > 0$ the non-standard model is favored over the ΛCDM whereas $\Delta{\rm DIC} < 0$ points out to a preference of the cosmological data for the standard model of cosmology. According to the usual standards, values $0 \le \Delta{\rm DIC} < 2$ would indicate *weak* evidence in favor of the non-standard model, if $2 \le \Delta{\rm DIC} < 6$ there would be *positive* evidence whereas for values in the range $6 \le \Delta{\rm DIC} < 10$ point out to *strong* preference for the cosmological extended model. Finally if we find values $\Delta{\rm DIC} > 10$ we are allowed to claim *very strong* evidence in favor of the non-standard model.

To check how consistent are, two sets of cosmological parameter constraints obtained with two different dataset, within a given model we use another statistical estimator based on the DIC values [63,88].

$$\mathcal{I}(D_1, D_2) \equiv \exp\left(-\frac{\mathcal{G}(D_1, D_2)}{2}\right) \tag{8}$$

where D_1 and D_2 are the two datasets under comparison and we define

$$\mathcal{G} = {\rm DIC}(D_1 \cup D_2) - {\rm DIC}(D_1) - {\rm DIC}(D_2). \tag{9}$$

This estimator is built in such a way that values $\log_{10}\mathcal{I} > 0$ indicate consistency between the results obtained with the two datasets whereas $\log_{10}\mathcal{I} < 0$ points to an inconsistency. According to Jeffrey's scale, we claim that the level of concordance/discordance is *inconclusive* if $|\log_{10}\mathcal{I}| < 0.5$, *substantial* if $|\log_{10}\mathcal{I}| > 0.5$, *strong* when $|\log_{10}\mathcal{I}| > 1$ and *decisive* for $|\log_{10}\mathcal{I}| > 2$.

4. Results

The cosmological parameter constraints obtained with the datasets: BAO + SNIa, PR4, PR4 + lensing, PR4 + BAO + SNIa and PR4 + lensing + BAO + SNIa for the models ΛCDM, ΛCDM + Ω_k, ΛCDM + A_L, w_0CDM and the w_0w_aCDM are provided in Tables 1,2,3,4 and 5 respectively. The corresponding two-dimensional contour plots can be seen in Figs. 1, 3, 2, 4 and 5.

The replacement of the PR3 CMB likelihood by the recent PR4 one brings significant changes in the results. The PR3 results displayed in this section are extracted from [55]. With the PR3 likelihood, when the ΛCDM + Ω_k is analyzed, a value of $\Omega_k = -0.044^{+0.018}_{-0.015}$ is obtained and the difference in the value of $\chi^2_{\rm min}$ with respect to the ΛCDM model is $\Delta\chi^2_{\rm min} = +11.36$. On the other hand, when we employ the PR4 likelihood to test the models, we obtain for the curvature model $\Omega_k = -0.0107^{+0.0096}_{-0.0080}$ and $\Delta\chi^2_{\rm min} = +3.80$. While both likelihoods still show preference for a closed universe, the significance of the results is different, being the first value 2.44σ away from $\Omega_k = 0$ whereas the second result favors non-flat spatial hypersurfaces by 1.11σ. For model-independent measurements of the curvature parameter Ω_k see [44] or alternative models [89] compatible with this result. In regard to the ΛCDM + A_L model, results along the same lines are obtained. When the PR3 data are analyzed, the favored value for the lensing parameter is $A_L = 1.180 \pm 0.065$ which deviates from $A_L = 1$ by 2.77σ being the difference in the minimum value of the χ^2-function with respect to the standard model $\Delta\chi^2_{\rm min} = +9.66$, whereas when the PR4 data are considered the results are $A_L = 1.036 \pm 0.055$ (0.65σ) and $\Delta\chi^2_{\rm min} = +2.53$. In light of these results one may claim that the so-called lensing anomaly is less significant once the PR3 likelihood is replaced in the analyses by the PR4 one. It is also interesting to see how the results change when the lensing data are added to the mix. In the case of the ΛCDM + Ω_k when the PR3 + lensing data are considered (being the lensing likelihood the one from PR3), the result obtained are $\Omega_k = -0.0106 \pm 0.065$ and $\Delta\chi^2_{\rm min} = +3.22$, representing a considerable reduction, when compared to the PR3 alone case, not only in the mild evidence in favor of a closed universe (1.63σ) but also in the better performance with respect to the standard model when it comes to fitting the data. As for the PR4 + lensing analysis we get $\Omega_k = -0.0073^{+0.0063}_{-0.0052}$ (1.16σ) and $\Delta\chi^2_{\rm min} = +1.99$, which indicates more stability in the results when we move from PR4 to PR4 + lensing data. A similar trend is observed in the ΛCDM + A_L but with some minor differences that are worth to be mentioned. While in the PR3 + lensing analysis the results are $A_L = 1.071^{+0.038}_{-0.042}$ (1.69σ) and $\Delta\chi^2_{\rm min} = +3.43$ in the PR4 + lensing case we have $A_L = 1.041 \pm 0.038$ (1.10σ) and $\Delta\chi^2_{\rm min} = +3.08$. Therefore, when PR3 data are considered there exists a clear decrease in the evidence in favor of $A_L > 1$ when the lensing data are included. However, when PR4 + lensing data are jointly analyzed, the option $A_L > 1$ is more favored in comparison with the case with only PR4 data. In regard to the dynamical dark energy parameterizations w_0CDM and w_0w_aCDM, even if the lensing data contains information about the late-time universe, either PR3 (PR4) or PR3 + lensing (PR4 + lensing), are not able to put tight constraints over the equation of state parameters and consequently no significant differences are appreciated when we move from PR3 to PR4.

For all the models under study we do not appreciate significant changes in the cosmological parameter constraints when we compare PR4 + BAO + SNIa results and PR4 + lensing + BAO + SNIa ones, therefore, we focus on the discussion of the results obtained with the second datasets since it is the most complete one. When the curvature paramater Ω_k is allowed to vary, we find for the ΛCDM + Ω_k model, $\Omega_k = 0.0018 \pm 0.0015$, indicating now a 1.2σ preference for an open universe. This somehow is in contradiction with the results obtained with PR4 for the same model, where a preference for a closed universe was found. This is reflected in the value $\log_{10}\mathcal{I} = -0.99$, obtained when we compare PR4 vs. BAO + SNIa results, which is on the verge of indicating a strong discordance between PR4 and BAO + SNIa results. This can also be seen by taking a look at Fig. 2 where non-overlaping contour plots at $\sim 2\sigma$ can be observed. In the comparison with the ΛCDM we observe a *positive* evidence in favor of the standard model. For the ΛCDM + A_L model, we get $A_L = 1.050 \pm 0.035$ which represents a deviation of 1.43σ with respect to the $A_L = 1$ expected value. The presence of the varying A_L parameter allows the model to slightly improve the performance of the ΛCDM $(\Delta\chi^2_{\rm min} = +2.10)$, however according to the DIC, $\Delta{\rm DIC} = +0.92$ the model is only *weakly* preferred over the standard model. As for the dynamical dark energy parameterizations we have for the w_0CDM, a value of the equation of state parameter $w_0 = -0.984 \pm 0.026$ which shows a 0.62σ deviation from the value $w_0 = -1$ associated to the cosmological constant. Which such small deviation with respect to the $w = -1$ this parameterization does not improve the ΛCDM fit. As expected the minimum value of the χ^2 function is below the one found for the ΛCDM, in particular $\Delta\chi^2_{\rm min} = +0.76$, however, when we penalize the presence of extra parameters $\Delta{\rm DIC} = -1.58$ it turns out that it is the standard model the one that is *weakly* preferred over the w_0CDM parameterization. According to the contour plots displayed in Fig. 4, there is tension between the cosmological parameter constraints obtained with PR4 and BAO + SNIa. This is also reflected in the value of the equation of state parameter, that points to a phantom behavior $w_0 = -1.51^{+0.18}_{-0.35}$ when PR4 data are analyzed and quintessence $w_0 = -0.978 \pm 0.026$ when PR4 + BAO + SNIa are jointly analyzed. However, this tension is not fully captured in the statistical estimator $\log_{10}\mathcal{I} = -0.15$, which is not conclusive. On the other hand, the w_0w_aCDM parameterization is favored when compared to the ΛCDM. For the equation of state parameters we obtain $w_0 = -0.843 \pm 0.062$ and $w_a = -0.64^{+0.29}_{-0.19}$. A more suitable parameter combination to check deviations from the ΛCDM $(w = -1)$ is $w_0 + w_a$, which is the value of the equation of

state in the limit of small values of a. If there is no deviation with respect to standard model then we should find $w_0 + w_a = -1$, but we get $w_0 + w_a = -1.48^{+0.23}_{-0.19}$ which is 2.1σ away from $w = -1$. We also obtain $\chi^2_{\rm min} = +5.31$ and $\Delta{\rm DIC} = +2.99$ which indicates that the w_0w_aCDM parameterization is *positively* favored when compared to the ΛCDM model. As for the concordance between PR4 and BAO + SNIa, according to the estimator employed in this work, we find $\log_{10}\mathcal{I} = 1.08$ pointing to a good agreement between the results obtained with the two datasets. It is interesting to note that similar results were found in [34,35,90], where PR3 and non-DESI data are used, which indicates that the results are stable regardless of the dataset considered. When using the same datasets and parameter extensions, our results are agree with the results in [59].

5. Conclusions

In this work we have tested some of the most common phenomenological extensions of the ΛCDM model in order to see whether they are capable of improving the performance of the standard model and we have reevaluated the status of the lensing anomaly by using PR4 CMB data and BAO DESI 2024 data. When PR3 data are replaced by PR4 data the evidence in favor of $\Omega_k < 0$ and $A_L > 1$ is clearly reduced. In particular we find $\Omega_k = -0.0107^{+0.0096}_{-0.0080}$ and $A_L = 1.036 \pm 0.055$ indicating a deviation of 1.11σ and 0.72σ from $\Omega_k = 0$ and $A_L = 1$, respectively. Therefore, we may claim that when PR4 data are analyzed the lensing anomaly almost subsides. Remarkably, the inclusion of the PR4-lensing data and the combination of BAO + SNIa increases the preference for non-flat spatial hypersurfaces ($\Omega_k = 0.0018 \pm 0.0015$) and for $A_L \neq 1$ ($A_L = 1.050 \pm 0.035$). When PR4 + lensing + BAO + SNIa data are analyzed, for the dynamical dark energy parameterization w_0CDM we find a slight shift (0.61σ) for a quintessence behavior $w_0 = -0.984 \pm 0.026$, however, according to the statistical criterion DIC, the model is *weakly* disfavored when compared to the ΛCDM. On the other hand for the w_0w_aCDM parameterization, when the same dataset is considered, we obtain $w_0 + w_a = -1.48^{+0.23}_{-0.19}$, which is separated by $\sim 2\sigma$ from the value expected $w_0 + w_a = -1$ in the standard model. In regard to the performance when it comes to fitting the data, we obtain $\Delta{\rm DIC} = +2.99$ indicating that the model is *positively* preferred over the ΛCDM model. Although these results are obtained within the context of a mere parameterization, this could serve as a clue to the behavior that the equation of state parameter, of more complex physical models, should follow in order to improve the performance of the standard model of cosmology.

CRediT authorship contribution statement

Jacobo Asorey: Writing – review & editing, Writing – original draft, Visualization, Validation, Resources, Project administration, Methodology, Investigation, Formal analysis, Data curation, Conceptualization; **Javier de Cruz Pérez:** Writing – review & editing, Writing – original draft, Visualization, Validation, Resources, Project administration, Methodology, Investigation, Formal analysis, Data curation, Conceptualization.

Data availability

The data used in the paper is public and referenced in it

Declaration of competing interest

The authors declare that they have no known competing financial interests or personal relationships that could have appeared to influence the work reported in this paper.

Acknowledgements

We would like to thank the insightful discussions with Guadalupe Cañas Herrera, Will Handley, Jesús Torrado and we would like to thank David Fernández Sanz for the help setting up the UCM computational facilities.

J. A. acknowledges the support of Universidad Complutense de Madrid UCM project PR3/23-30808, Spanish MINECO/FEDER Grants No. PGC2022-126078NB- C21 funded by MCIN/AEI/10.13039/50110001103 and DGA-FSE grant 2023-E21-23R. JdCP's research was financially supported by the project "Plan Complementario de I + D + i en el área de Astrofísica" funded by the European Union within the framework of the Recovery, Transformation and Resilience Plan - NextGenerationEU and by the Regional Government of Andalucía (Reference AST22_00001). Both J. A and J. dCP acknowledge partial support from MICINN (Spain) project PID2022-138263NB-I0 (AEI/FEDER, UE). Both authors acknowledge participation in the Cost Association Action CA21136 "Addressing observational tensions in cosmology with systematics and fundamental physics (CosmoVerse)" This project has been done by using the resources of the `Aljuarismi` computing facility of the Facultad de Ciencias Físicas of Universidad Complutense de Madrid. We acknowledge the use of the computational resources of CESAR at BIFI Institute (University of Zaragoza), in particular, the facility `Agustina`. We wish to ackowledge the use of the `Cobaya` library [76,91] for the production of the MCMC chains.

References

[1] G. Hinshaw, et al., WMAP, Nine-Year Wilkinson Microwave Anisotropy Probe (WMAP) observations: cosmological parameter results, Astrophys. J. Suppl. 208 (2013) 19. arXiv:1212.5226, https://doi.org/10.1088/0067-0049/208/2/19
[2] N. Aghanim, et al., Planck, Planck 2018 results. VI. Cosmological parameters, Astron. Astrophys. 641 (2020) A6. [Erratum: Astron.Astrophys. 652, C4 (2021)]. arXiv:1807.06209, https://doi.org/10.1051/0004-6361/201833910
[3] T. Louis, et al., ACT, The Atacama Cosmology Telescope: DR6 power spectra, likelihoods and LCDM parameters (2025). arXiv:2503.14452
[4] M. Betoule, et al., SDSS, Improved cosmological constraints from a joint analysis of the SDSS-II and SNLS supernova samples, Astron. Astrophys. 568 (2014) A22. arXiv:1401.4064, https://doi.org/10.1051/0004-6361/201423413
[5] D. Brout, et al., The Pantheon+ analysis: cosmological constraints, Astrophys. J. 938 (2) (2022) 110. arXiv:2202.04077, https://doi.org/10.3847/1538-4357/ac8e04
[6] D. Rubin, et al., Union through UNITY: cosmology with 2,000 SNe using a unified bayesian framework (2023). arXiv:2311.12098
[7] T.M.C. Abbott, et al., DES, The Dark Energy Survey: cosmology results with ~1500 new high-redshift type ia supernovae using the full 5 yr data set, Astrophys. J. Lett. 973 (1) (2024) L14. arXiv:2401.02929, https://doi.org/10.3847/2041-8213/ad6f9f
[8] W.J. Percival, et al., 2dFGRS, The 2dF galaxy redshift survey: the power spectrum and the matter content of the universe, Mon. Not. Roy. Astron. Soc. 327 (2001) 1297. arXiv:astro-ph/0105252, https://doi.org/10.1046/j.1365-8711.2001.04827.x
[9] D.J. Eisenstein, et al., SDSS, Detection of the baryon acoustic peak in the large-Scale correlation function of SDSS luminous red galaxies, Astrophys. J. 633 (2005) 560–574. arXiv:astro-ph/0501171, https://doi.org/10.1086/466512
[10] E. Gaztanaga, A. Cabre, L. Hui, Clustering of luminous red galaxies IV: baryon acoustic peak in the line-of-Sight direction and a direct measurement of H(z), Mon. Not. Roy. Astron. Soc. 399 (2009) 1663–1680. arXiv:0807.3551, https://doi.org/10.1111/j.1365-2966.2009.15405.x
[11] C. Blake, et al., The WiggleZ dark energy survey: testing the cosmological model with baryon acoustic oscillations at z = 0.6, Mon. Not. Roy. Astron. Soc. 415 (2011) 2892–2909. arXiv:1105.2862, https://doi.org/10.1111/j.1365-2966.2011.19077.x
[12] F. Beutler, C. Blake, M. Colless, D.H. Jones, L. Staveley-Smith, L. Campbell, Q. Parker, W. Saunders, F. Watson, The 6dF galaxy survey: baryon acoustic oscillations and the local hubble constant, Mon. Not. Roy. Astron. Soc. 416 (2011) 3017–3032. arXiv:1106.3366, https://doi.org/10.1111/j.1365-2966.2011.19250.x
[13] S. Alam, et al., eBOSS, Completed SDSS-IV extended Baryon Oscillation Spectroscopic Survey: cosmological implications from two decades of spectroscopic surveys at the Apache Point observatory, Phys. Rev. D 103 (8) (2021) 083533. arXiv:2007.08991, https://doi.org/10.1103/PhysRevD.103.083533
[14] A.G. Adame, et al., DESI, DESI 2024 VI: Cosmological constraints from the measurements of baryon acoustic oscillations, arXiv:2404.03002 (2024).
[15] T.M.C. Abbott, et al., DES, Dark Energy Survey year 1 results: cosmological constraints from galaxy clustering and weak lensing, Phys. Rev. D 98 (4) (2018) 043526. arXiv:1708.01530, https://doi.org/10.1103/PhysRevD.98.043526
[16] M. Asgari, et al., KiDS, KiDS-1000 cosmology: cosmic shear constraints and comparison between two point statistics, Astron. Astrophys. 645 (2021) A104. arXiv:2007.15633, https://doi.org/10.1051/0004-6361/202039070
[17] T.M.C. Abbott, et al., DES, Dark Energy Survey year 3 results: cosmological constraints from galaxy clustering and weak lensing, Phys. Rev. D 105 (2) (2022) 023520. arXiv:2105.13549, https://doi.org/10.1103/PhysRevD.105.023520

[18] A.J. Cuesta, L. Verde, A. Riess, R. Jimenez, Calibrating the cosmic distance scale ladder: the role of the sound horizon scale and the local expansion rate as distance anchors, Mon. Not. Roy. Astron. Soc. 448 (4) (2015) 3463–3471. arXiv:1411.1094, https://doi.org/10.1093/mnras/stv261

[19] J.L. Bernal, L. Verde, A.G. Riess, The trouble with H_0, JCAP 10 (2016) 019. arXiv:1607.05617 https://doi.org/10.1088/1475-7516/2016/10/019

[20] L. Verde, T. Treu, A.G. Riess, Tensions between the early and the late universe, Nature Astron. 3 (2019) 891. arXiv:1907.10625, https://doi.org/10.1038/s41550-019-0902-0

[21] E. Di Valentino, O. Mena, S. Pan, L. Visinelli, W. Yang, A. Melchiorri, D.F. Mota, A.G. Riess, J. Silk, In the realm of the Hubble tension—a review of solutions, Class. Quant. Grav. 38 (15) (2021) 153001. arXiv:2103.01183, https://doi.org/10.1088/1361-6382/ac086d

[22] O.T. Oayda, V. Mittal, G.F. Lewis, T. Murphy, A bayesian approach to the cosmic dipole in radio galaxy surveys: joint analysis of NVSS & RACS, Mon. Not. Roy. Astron. Soc. 531 (4) (2024) 4545–4559. arXiv:2406.01871, https://doi.org/10.1093/mnras/stae1399

[23] S.-F. Chen, M. White, J. DeRose, N. Kokron, Cosmological analysis of three-dimensional BOSS galaxy clustering and Planck CMB lensing cross correlations via lagrangian perturbation theory, JCAP 07 (07) (2022) 041. arXiv:2204.10392, https://doi.org/10.1088/1475-7516/2022/07/041

[24] S. Anselmi, P.-S. Corasaniti, A.G. Sanchez, G.D. Starkman, R.K. Sheth, I. Zehavi, Cosmic distance inference from purely geometric BAO methods: linear point standard ruler and correlation function model fitting, Phys. Rev. D 99 (12) (2019) 123515. arXiv:1811.12312, https://doi.org/10.1103/PhysRevD.99.123515

[25] A. Favale, A. Gómez-Valent, M. Migliaccio, Quantification of 2D vs 3D BAO tension using SNIa as a redshift interpolator and test of the etherington relation, Phys. Lett. B 858 (2024) 139027. arXiv:2405.12142, https://doi.org/10.1016/j.physletb.2024.139027

[26] M. Abdul Karim, et al., DESI, DESI DR2 Results II: measurements of baryon acoustic oscillations and cosmological constraints (2025). arXiv:2503.14738

[27] T.M.C. Abbott, et al., DES, Dark Energy Survey: a 2.1the angular baryonic acoustic oscillation scale at redshift zeff = 0.85 from the final dataset, Phys. Rev. D 110 (6) (2024) 063515. arXiv:2402.10696, https://doi.org/10.1103/PhysRevD.110.063515

[28] T.M.C. Abbott, et al., DES, Dark Energy Survey: implications for cosmological expansion models from the final DES baryon acoustic oscillation and supernova data (2025). arXiv:2503.06712

[29] J. Sola, A. Gomez-Valent, J. de Cruz Pérez, Hints of dynamical vacuum energy in the expanding universe, Astrophys. J. Lett. 811 (2015) L14. arXiv:1506.05793, https://doi.org/10.1088/2041-8205/811/1/L14

[30] J. Solà, A. Gómez-Valent, J. de Cruz Pérez, First evidence of running cosmic vacuum: challenging the concordance model, Astrophys. J. 836 (1) (2017) 43. arXiv:1602.02103, https://doi.org/10.3847/1538-4357/836/1/43

[31] J. Solà Peracaula, J. de Cruz Pérez, A. Gómez-Valent, Dynamical dark energy vs. Λ = const in light of observations, EPL 121 (3) (2018) 39001. arXiv:1606.00450, https://doi.org/10.1209/0295-5075/121/39001

[32] J. Solà Peracaula, J. de Cruz Pérez, A. Gomez-Valent, Possible signals of vacuum dynamics in the universe, Mon. Not. Roy. Astron. Soc. 478 (4) (2018) 4357–4373. arXiv:1703.08218 https://doi.org/10.1093/mnras/sty1253

[33] G.-B. Zhao, et al., Dynamical dark energy in light of the latest observations, Nature Astron. 1 (9) (2017) 627–632. arXiv:1701.08165, https://doi.org/10.1038/s41550-017-0216-z

[34] C.-G. Park, J. de Cruz Pérez, B. Ratra, Using non-DESI data to confirm and strengthen the DESI 2024 spatially flat w0waCDM cosmological parametrization result, Phys. Rev. D 110 (12) (2024) 123533. arXiv:2405.00502 https://doi.org/10.1103/PhysRevD.110.123533

[35] C.-G. Park, J. de Cruz Pérez, B. Ratra, Is the w_0w_aCDM cosmological parameterization evidence for dark energy dynamics partially caused by the excess smoothing of Planck CMB anisotropy data? (2024). arXiv:2410.13627

[36] A. Gomez-Valent, J. Solà Peracaula, Phantom matter: a challenging solution to the cosmological tensions, Astrophys. J. 975 (1) (2024) 64. arXiv:2404.18845, https://doi.org/10.3847/1538-4357/ad7a62

[37] L. Perivolaropoulos, F. Skara, Challenges for ΛCDM: an update, New Astron. Rev. 95 (2022) 101659. arXiv:2105.05208, https://doi.org/10.1016/j.newar.2022.101659

[38] E. Abdalla, et al., Cosmology intertwined: a review of the particle physics, astrophysics, and cosmology associated with the cosmological tensions and anomalies, JHEAp 34 (2022) 49–211. arXiv:2203.06142 https://doi.org/10.1016/j.jheap.2022.04.002

[39] P.J.E. Peebles, Anomalies in physical cosmology, Annals Phys. 447 (2022) 169159. arXiv:2208.05018, https://doi.org/10.1016/j.aop.2022.169159

[40] E. Di Valentino, et al., CosmoVerse, The CosmoVerse white paper: addressing observational tensions in cosmology with systematics and fundamental physics (2025). arXiv:2504.01669

[41] B. L'Huillier, A. Shafieloo, Model-independent test of the FLRW metric, the flatness of the universe, and non-local measurement of H_0r_d, JCAP 01 (2017) 015. arXiv:1606.06832 https://doi.org/10.1088/1475-7516/2017/01/015

[42] A. Shafieloo, B. L'Huillier, A.A. Starobinsky, Falsifying ΛCDM: model-independent tests of the concordance model with eBOSS DR14Q and Pantheon, Phys. Rev. D 98 (8) (2018) 083526. arXiv:1804.04320, https://doi.org/10.1103/PhysRevD.98.083526

[43] B. L'Huillier, A. Mitra, A. Shafieloo, R.E. Keeley, H. Koo, Litmus tests of the flat ΛCDM model and model-independent measurement of H_0 r_d with LSST and DESI, JCAP 05 (2025) 030. arXiv:2407.07847 https://doi.org/10.1088/1475-7516/2025/05/030

[44] A. Favale, A. Gómez-Valent, M. Migliaccio, Cosmic chronometers to calibrate the ladders and measure the curvature of the universe. a model-independent study, Mon. Not. Roy. Astron. Soc. 523 (3) (2023) 3406–3422. arXiv:2301.09591, https://doi.org/10.1093/mnras/stad1621

[45] A.G. Riess, et al., A comprehensive measurement of the local value of the Hubble constant with 1 km/s/mpc uncertainty from the hubble space telescope and the SH0ES team, Astrophys. J. Lett. 934 (1) (2022) L7. arXiv:2112.04510, https://doi.org/10.3847/2041-8213/ac5c5b

[46] W.L. Freedman, B.F. Madore, I.S. Jang, T.J. Hoyt, A.J. Lee, K.A. Owens, Status report on the Chicago-Carnegie Hubble program (CCHP): three independent astrophysical determinations of the Hubble constant using the James Webb Space Telescope (2024). arXiv:2408.06153

[47] B.P. Abbott, et al., LIGO Scientific, Virgo, 1M2H, Dark Energy Camera GW-E, DES, DLT40, Las Cumbres Observatory, VINROUGE, MASTER, A gravitational-wave standard siren measurement of the Hubble constant, Nature 551 (7678) (2017) 85–88. arXiv:1710.05835, https://doi.org/10.1038/nature24471

[48] K.C. Wong, et al., H0LiCOW, H0LiCOW – XIII. A 2.4 per cent measurement of H0 from lensed quasars: 5.3σ tension between early- and late-Universe probes, Mon. Not. Roy. Astron. Soc. 498 (1) (2020) 1420–1439. arXiv:1907.04869, https://doi.org/10.1093/mnras/stz3094

[49] S. Birrer, et al., TDCOSMO 2025: Cosmological constraints from strong lensing time delays, in: 3rd General Meeting of CosmoVerse: Addressing Observational Tensions in Cosmology with Systematics and Fundamental Physics, 2025. arXiv:2506.03023

[50] G. Risaliti, E. Lusso, A Hubble diagram for quasars, Astrophys. J. 815 (2015) 33. arXiv:1505.07118, https://doi.org/10.1088/0004-637X/815/1/33

[51] E. Lusso, et al., Quasars as standard candles III. validation of a new sample for cosmological studies, Astron. Astrophys. 642 (2020) A150. arXiv:2008.08586, https://doi.org/10.1051/0004-6361/202038899

[52] J.A. Hodgson, B. L'Huillier, I. Liodakis, S.-S. Lee, A. Shafieloo, Using variability and VLBI to measure cosmological distances, Mon. Not. Roy. Astron. Soc. 495 (1) (2020) L27–L31. arXiv:2003.10278, https://doi.org/10.1093/mnrasl/slaa051

[53] J.A. Hodgson, B. L'Huillier, I. Liodakis, S.-S. Lee, A. Shafieloo, Estimating the feasibility of 'standard speed-gun' distances, Mon. Not. Roy. Astron. Soc. 521 (1) (2023) L44–L47. arXiv:2301.06252, https://doi.org/10.1093/mnrasl/slad007

[54] E. Calabrese, A. Slosar, A. Melchiorri, G.F. Smoot, O. Zahn, Cosmic microwave weak lensing data as a test for the dark universe, Phys. Rev. D 77 (2008) 123531. arXiv:0803.2309, https://doi.org/10.1103/PhysRevD.77.123531

[55] P. Collaboration, Planck 2018 Results: Cosmological Parameter Tables, https://wiki.cosmos.esa.int/planck-legacy-archive/images/9/9c/Baseline_params_table_2018_95pc.pdf, 2018, https://wiki.cosmos.esa.int/planck-legacy-archive/images/4/43/Baseline_params_table_2018_68pc_v2.pdf.

[56] Y. Akrami, et al., Planck, *Planck* Intermediate results. LVII. joint planck LFI and HFI data processing, Astron. Astrophys. 643 (2020) A42. arXiv:2007.04997, https://doi.org/10.1051/0004-6361/202038073

[57] E. Rosenberg, S. Gratton, G. Efstathiou, CMB Power spectra and cosmological parameters from Planck PR4 with camspec, Mon. Not. Roy. Astron. Soc. 517 (3) (2022) 4620–4636. arXiv:2205.10869, https://doi.org/10.1093/mnras/stac2744

[58] M. Tristram, et al., Cosmological parameters derived from the final Planck data release (PR4), Astron. Astrophys. 682 (2024) A37. arXiv:2309.10034, https://doi.org/10.1051/0004-6361/202348015

[59] S. Roy Choudhury, T. Okumura, Updated cosmological constraints in extended parameter space with Planck PR4, DESI baryon acoustic oscillations, and supernovae: dynamical dark energy, neutrino masses, lensing anomaly, and the Hubble tension, Astrophys. J. Lett. 976 (1) (2024) L11. arXiv:2409.13022, https://doi.org/10.3847/2041-8213/ad8c26

[60] S. Roy Choudhury, Cosmology in extended parameter space with DESI data release 2 baryon acoustic oscillations: a $2\sigma+$ detection of nonzero neutrino masses with an update on dynamical dark energy and lensing anomaly, Astrophys. J. Lett. 986 (2025) L31. arXiv:2504.15340, https://doi.org/10.3847/2041-8213/ade1cc

[61] J. Carron, M. Mirmelstein, A. Lewis, CMB Lensing from Planck PR4 maps, JCAP 09 (2022) 039. arXiv:2206.07773 https://doi.org/10.1088/1475-7516/2022/09/039

[62] A. Gómez-Valent, J. Solà Peracaula, Composite dark energy and the cosmological tensions, Phys. Lett. B 864 (2025) 139391. arXiv:2412.15124, https://doi.org/10.1016/j.physletb.2025.139391

[63] J. de Cruz Perez, C.-G. Park, B. Ratra, Current data are consistent with flat spatial hypersurfaces in the ΛCDM cosmological model but favor more lensing than the model predicts, Phys. Rev. D 107 (6) (2023) 063522. arXiv:2211.04268, https://doi.org/10.1103/PhysRevD.107.063522

[64] S. Sanz-Wuhl, H. Gil-Marín, A.J. Cuesta, L. Verde, BAO Cosmology in non-spatially flat background geometry from BOSS + eBOSS and lessons for future surveys, JCAP 05 (2024) 116. arXiv:2402.03427 https://doi.org/10.1088/1475-7516/2024/05/116

[65] W. Hu, Weak lensing of the CMB: a harmonic approach, Phys. Rev. D 62 (2000) 043007. arXiv:astro-ph/0001303, https://doi.org/10.1103/PhysRevD.62.043007

[66] A. Lewis, A. Challinor, Weak gravitational lensing of the CMB, Phys. Rept. 429 (2006) 1–65. arXiv:astro-ph/0601594, https://doi.org/10.1016/j.physrep.2006.03.002

[67] M. Chevallier, D. Polarski, Accelerating universes with scaling dark matter, Int. J. Mod. Phys. D 10 (2001) 213–224. arXiv:gr-qc/0009008, https://doi.org/10.1142/S0218271801000822

[68] E.V. Linder, Exploring the expansion history of the universe, Phys. Rev. Lett. 90 (2003) 091301. arXiv:astro-ph/0208512, https://doi.org/10.1103/PhysRevLett.90.091301

[69] X. Li, A. Shafieloo, A simple phenomenological emergent dark energy model can resolve the Hubble tension, Astrophys. J. Lett. 883 (1) (2019) L3. arXiv:1906.08275, https://doi.org/10.3847/2041-8213/ab3e09
[70] C.-G. Park, B. Ratra, Is excess smoothing of Planck CMB ansiotropy data partially responsible for evidence for dark energy dynamics in other $w(z)$CDM parametrizations? (2025). arXiv:2501.03480
[71] K. Lodha, et al., DESI, Extended dark energy analysis using DESI DR2 BAO measurements (2025). arXiv:2503.14743
[72] A. González-Fuentes, A. Gómez-Valent, Reconstruction of dark energy and late-time cosmic expansion using the weighted function regression method (2025). arXiv:2506.11758
[73] E.Ó. Colgáin, S. Pourojaghi, M.M. Sheikh-Jabbari, L. Yin, How much has DESI dark energy evolved since DR1? (2025). arXiv:2504.04417
[74] J. Lesgourgues, The cosmic linear anisotropy solving system (CLASS) i: overview, arXiv:1104.2932 (2011). https://lesgourg.github.io/class_public/class.html.
[75] D. Blas, J. Lesgourgues, T. Tram, The cosmic linear anisotropy solving system (CLASS) II: approximation schemes, JCAP 1107 (2011) 034. arXiv:1104.2933, https://doi.org/10.1088/1475-7516/2011/07/034
[76] J. Torrado, A. Lewis, Cobaya: code for bayesian analysis of hierarchical physical models, JCAP 05 (2021) 057. arXiv:2005.05290 https://doi.org/10.1088/1475-7516/2021/05/057
[77] S.P. Brooks, A. Gelman, General methods for monitoring convergence of iterative simulations, J. Comput. Graph. Stat. 7 (1997) 434. https://doi.org/10.1080/10618600.1998.10474787
[78] A. Gelman, D.B. Rubin, Inference from iterative simulation using multiple sequences, Stat. Sci. 7 (1992) 457. https://doi.org/10.1214/SS/1177011136
[79] A. Lewis, Getdist: a python package for analysing monte carlo samples (2019). arXiv:1910.13970
[80] A.G. Sanchez, Arguments against using h^{-1}Mpc units in observational cosmology, Phys. Rev. D 102 (12) (2020) 123511. arXiv:2002.07829, https://doi.org/10.1103/PhysRevD.102.123511
[81] M. Forconi, A. Favale, A. Gómez-Valent, Illustrating the consequences of a misuse of σ_8 in cosmology (2025). arXiv:2501.11571
[82] D.J. Fixsen, The temperature of the cosmic microwave background, Astrophys. J. 707 (2009) 916–920. arXiv:0911.1955. https://doi.org/10.1088/0004-637X/707/2/916
[83] D.J. Spiegelhalter, N.G. Best, B.P. Carlin, A. van der Linde, Bayesian measures of model complexity and fit, J. Roy. Stat. Soc. 64 (2002) 583. https://doi.org/10.1111/1467-9868.00353
[84] M. Kunz, R. Trotta, D. Parkinson, Measuring the effective complexity of cosmological models, Phys. Rev. D 74 (2006) 023503. arXiv:astro-ph/0602378, https://doi.org/10.1103/PhysRevD.74.023503
[85] A.R. Liddle, Information criteria for astrophysical model selection, Mon. Not. Roy. Astron. Soc. 377 (2007) L74–L78. arXiv:astro-ph/0701113, https://doi.org/10.1111/j.1745-3933.2007.00306.x
[86] C. Cartis, J. Fiala, B. Marteau, L. Roberts, Improving the flexibility and robustness of model-Based derivative-Free optimization solvers (2018). arXiv:1804.00154
[87] C. Cartis, L. Roberts, O. Sheridan-Methven, Escaping local minima with local derivative-free methods: a numerical investigation, Optimization 71 (8) (2021) 2343–2373. arXiv:1812.11343, https://doi.org/10.1080/02331934.2021.1883015
[88] S. Joudaki, et al., CFHTLenS revisited: assessing concordance with Planck including astrophysical systematics, Mon. Not. Roy. Astron. Soc. 465 (2) (2017) 2033–2052. arXiv:1601.05786, https://doi.org/10.1093/mnras/stw2665
[89] W.-N. Deng, W. Handley, Predicting spatial curvature Ω_K in globally CPT-symmetric universes, Phys. Rev. D 110 (10) (2024) 103528. arXiv:2407.18225, https://doi.org/10.1103/PhysRevD.110.103528
[90] J. de Cruz Perez, C.-G. Park, B. Ratra, Updated observational constraints on spatially flat and nonflat ΛCDM and XCDM cosmological models, Phys. Rev. D 110 (2) (2024) 023506. arXiv:2404.19194, https://doi.org/10.1103/PhysRevD.110.023506
[91] J. Torrado, A. Lewis, Cobaya: bayesian analysis in cosmology, Astrophys. Source Code Lib., record ascl:1910.019, 2019 https://ui.adsabs.harvard.edu/abs/2019ascl.soft10019T.